



Heriot-Watt University
Research Gateway

Photovoltaic effect and photopolarization in Pb [(Mg^{1/3}Nb^{2/3})_{0.68}Ti_{0.32}]O₃ crystal

Citation for published version:

Makhort, AS, Chevrier, F, Kundys, D, Doudin, B & Kundys, B 2018, 'Photovoltaic effect and photopolarization in Pb [(Mg^{1/3}Nb^{2/3})_{0.68}Ti_{0.32}]O₃ crystal', *Physical Review Materials*, vol. 2, no. 1, 012401. <https://doi.org/10.1103/PhysRevMaterials.2.012401>

Digital Object Identifier (DOI):

[10.1103/PhysRevMaterials.2.012401](https://doi.org/10.1103/PhysRevMaterials.2.012401)

Link:

[Link to publication record in Heriot-Watt Research Portal](#)

Document Version:

Peer reviewed version

Published In:

Physical Review Materials

General rights

Copyright for the publications made accessible via Heriot-Watt Research Portal is retained by the author(s) and / or other copyright owners and it is a condition of accessing these publications that users recognise and abide by the legal requirements associated with these rights.

Take down policy

Heriot-Watt University has made every reasonable effort to ensure that the content in Heriot-Watt Research Portal complies with UK legislation. If you believe that the public display of this file breaches copyright please contact open.access@hw.ac.uk providing details, and we will remove access to the work immediately and investigate your claim.

Photovoltaic effect and photopolarization in $\text{Pb}[(\text{Mg}_{1/3}\text{Nb}_{2/3})_{0.68}\text{Ti}_{0.32}]\text{O}_3$ crystals

A.S. Makhort¹, F. Chevrier¹, D. Kundys², B. Doudin¹, B. Kundys¹

² *Institute de Physique et de Chimie des Matériaux de Strasbourg, UMR 7504 CNRS-ULP, 23 rue du Loess, BP 43, F67034 Strasbourg Cedex 2, France*

¹ *Scottish Universities Physics Alliance (SUPA), Institute of Photonics and Quantum Sciences, School of Engineering and Physical Sciences, Heriot-Watt University, Edinburgh EH14 4AS, UK.*

Abstract

Ferroelectric photovoltaic materials offer an alternative to modern photovoltaic development by overcoming the bandgap limitations. However, the number of known compounds and photovoltaic efficiencies remain low. Here, we report the discovery of a photovoltaic effect in the undoped lead magnesium niobate – lead titanate crystal and a significant improvement in the photovoltaic response under properly chosen electric fields and temperatures. The photovoltaic (PV) effect is maximal near the electric-field-driven ferroelectric (FE) dipole reorientation and also increases by over 3 fold near FE T_c . Moreover, at FE saturation, the photovoltaic response clearly exhibits remanent and transient effects. The combination of such tuning possibility together with transient-remanent variations establishes photoferroelectric crystals as emerging elements for photovoltaicity and optoelectronics, with particular relevance to the all-optical storage and information processing.

Photoferroelectric compounds are remarkable materials having large potential for multi-functional applications¹. These materials that exhibit (multi)ferroic order are of particular interest, mainly because they offer an advanced electric operation related to multiple electric polarization switching states. Attention to photoferroelectrics has rejuvenated after the discovery of the photovoltaic effect in the multiferroic BiFeO₃^{2,3}, resulting in the revival of ferroelectric-based photovoltaic operation of related materials^{4,5,6,7,8}. Based on recent progress in photovoltaic efficiency in the Bi₂FeCrO₆ films⁹, FE cells are likely to become the actual competitors of the conventional photovoltaics in the nearest future. In this respect, having a better insight into photo-induced changes of electrical properties over the wide temperature range and electric fields is of crucial importance. Such study, however, requires high-quality crystals that are free from extrinsic contributions related to the surface/interface effects⁵ and grain size dependence¹⁰. This task is challenging because, the total number of currently known photovoltaic-ferroelectric compounds is well below 20^{5,11}. In this work, we consider the ferroelectric material of so-called PMN–PT family with the general formula of Pb[Mg_{1/3}Nb_{2/3}]_xTi_{1-x}]O₃. Based on the analogy with WO₃-doped PLZT (Pb_{1-x}La_x(Zr_yTi_z)_{1-x/4}O₃) ceramics¹², such WO₃ doping procedure was reported to introduce photovoltaic effect also in the Pb(Mg_{1/3}Nb_{2/3})_{0.64}Ti_{0.36}O₃ (PMN-PT 36%) single crystal¹³. In this work, we report that the photovoltaic effect exists even in the undoped compound of the same family, namely in the widely available Pb[(Mg_{1/3}Nb_{2/3})_xTi_{1-x}]O₃ (PMN–32%PT) composition¹⁴. We also detail for the first time remanent photo-polarization properties originating from photo-carrier generation-distribution mechanism. We further demonstrate how photovoltaic response can be tuned by varying the temperature and applied electric field.

Figure 1 represents the ferroelectric (FE) properties of the sample in darkness and under illumination aligned along the smallest direction [001] (inset). The FE loop measured in darkness reveals a classical hysteresis loop behavior resulting in three polarization states: the spontaneous ('0'), and two saturated states with opposite polarization ('1' and '2'). Light irradiation induces a large change in the FE loop. The sample evidently becomes leakier FE with apparent increase in the both FE polarization and FE coercive force (Fig.1b). This is also confirmed by the corresponding FE current in the Fig. 1c.

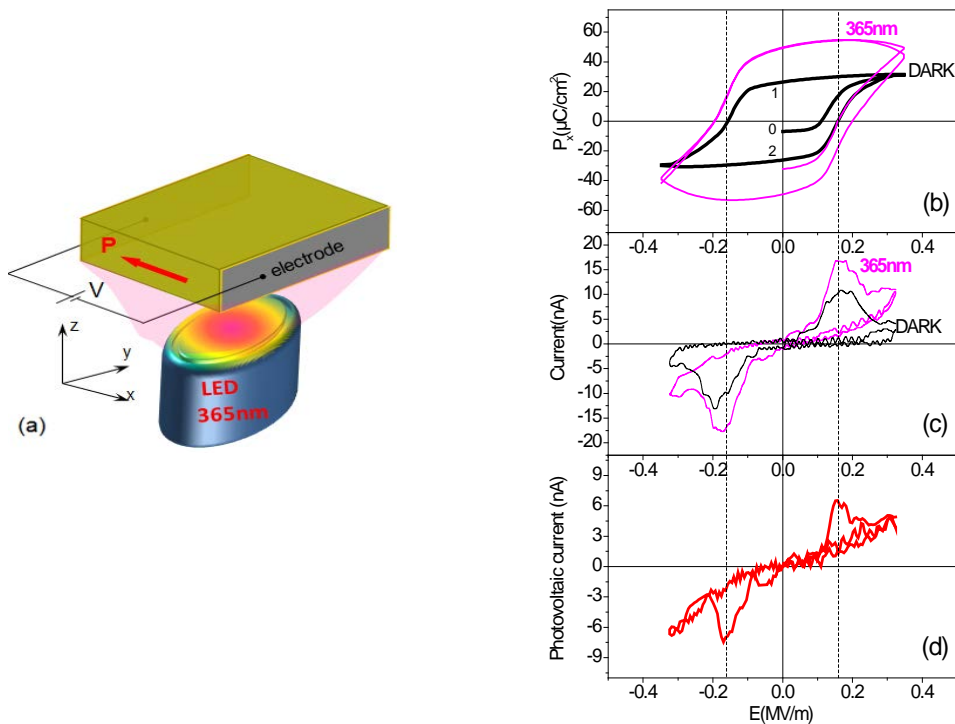


Figure 1 | Photoferroelectric measurements details. (a) Schematic of the experiment setup with respect to the crystalline axis. Ferroelectric polarization (b) and current (c) hysteresis loops in darkness and under 365nm irradiation. (c) Related photocurrent as a function of voltage.

The difference between the current under the illumination and the current in darkness (Fig.1d) corresponds to the photocurrent in the material, and reveals at least two important features. The first one is that the photocurrent, and therefore the bulk photovoltaic effect, strongly depends on the ferroelectric state so far reported for thin films as a function of wavelength only^{15,16}. The electric field-dependent measurements performed here on single crystals, free from extrinsic contributions, evidently detail the poling history dependence of the purely bulk photovoltaic effect. Secondly, this behavior, clearly illustrated here for the first time, reveals that the maximum of the photocurrent is observed at the electric field corresponding to the FE dipole reorientation. Such induced photocurrent should be able to impact the remanent FE state as recently reported by Iurchuk et al^{Error! Bookmark not defined.}. The time dependence of the related photopolarization measured at the three FE states (0, 1 and 2) shown in fig.2 provides insight into the mechanism explaining how photopolarization properties relate to the ferroelectric state of the material. For a sample initially polarized positively (FE state ‘1’) the

illumination generates charges which distribute along the previously forced polarization direction [100].

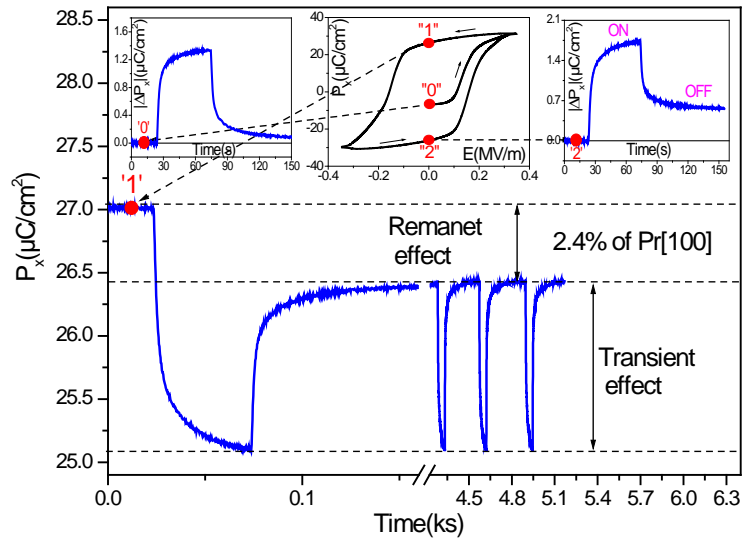


Figure 2 | Photopolarization effect. A sample initially in remnant state ‘1’, is illuminated by a UV (365 nm) diode. Within a few s, a change of polarization is established, with a fraction remaining after turning off the light (remanent effect). Subsequent illuminations only reveal the transient effect, with no more remanence. Insets show how the remanence in polarization depends on the FE state.

The photocarriers diminish surface charges, and therefore decrease the internal electric field of the material and the sample polarization. After turning the light OFF, charge trapping makes this decrease partially persisting (remanent effect, Fig. 2), leaving the sample in a slightly reduced remanent polarization state. Subsequent illumination pulses reveal only a transient effect as they are of the same energy and the ‘saturation’ of the remanence had been already achieved. Notably the initial polarization state can be recovered electrically by moving the ferroelectric system to the point “1” again. Similar effect, but with a different sign is observed for the ferroelectric point ‘2’, as it would be expected from the 180° symmetrical polarization rotation. In confirmation of the photo-carriers distribution scenario driven by an internal electric field, no significant remanence is observed for the spontaneous state ‘0’ which is close to the sample depolarization along the given [100] direction (figure 2 (left inset)). The gain in the photopolarization G_{hv} can be determined from our measurements as a relation of the number of photoexcited electrons (N_e) to the number of photons (N_{hv}):

$$G_{hv} = \frac{N_e}{N_{hv}} \quad (1)$$

The related gain is about 2.76ppm calculated for the transient part of the photopolarization for the wavelength of 365nm (Fig.2) and is about 30% larger for the remanent part. Insight into the temperature dependence of the photoelectric performance can be obtained from Figs. 3 and 4.

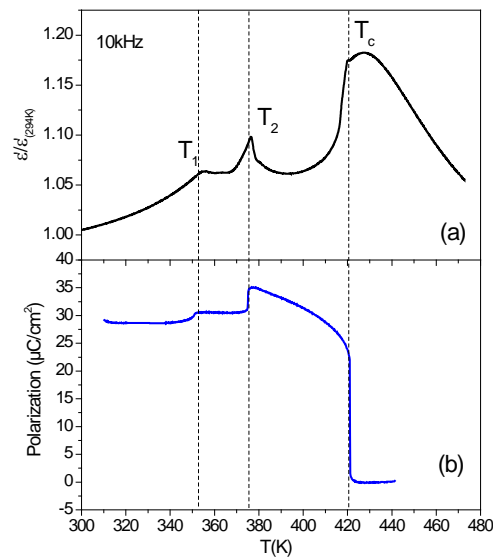


Figure 3 | Temperature dependence of the dielectric permittivity (a) and polarization (b) in darkness.

The sample was first warmed in darkness above its Curie temperature T_c (~ 421 K) and then cooled under applied electric field of 2.37kV/cm. The electric field was then set to zero and dielectric permittivity (fig.3b) was measured during warming above the T_c . The same procedure was applied to measure the electric polarization (fig.3b). The three characteristic transitions at T_1 , T_2 and T_c are clearly observed. While T_2 and T_c are related to the rhombohedral-tetragonal and the tetragonal-cubic transitions¹⁷ respectively the domain structure-related anomaly at T_1 appears as a function of poling¹⁸. Taking into account that light can modify the transition temperatures^{19,20,21}, the open-circuit photovoltage was measured for several temperatures, keeping in mind the abovementioned critical points where anomalies in the electric properties are observed. The results in figure 4 show that even at room temperature the transient part of photovoltage manifests more than one order of magnitude larger spectral efficiency than for previously reported for WO_3 -doped crystal¹¹. The photovoltaic isotherms reveal nonlinear behavior as a function of light intensity with the peak near 53mW/cm². This effect excellently confirms the two competing mechanisms: light induced charge generation (for intensities $\leq 53\text{mW}/\text{cm}^2$) and charge recombination process (for intensities $\geq 53\text{mW}/\text{cm}^2$).

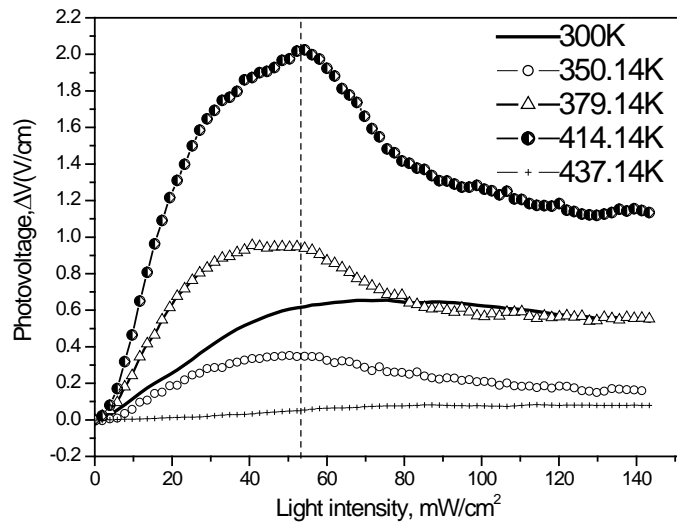


Figure 4 | Open circuit transient photovoltage isotherms as a function of light intensity.

The both processes opposing each other give the peak as a function of light intensity near 53mW/cm^2 where the number of generated and recombined carriers becomes comparable. Because of nonlinear character of the effect the maximal photovoltaic change has been extracted from the photovoltaic isotherms and is plotted against temperature in figure 5.

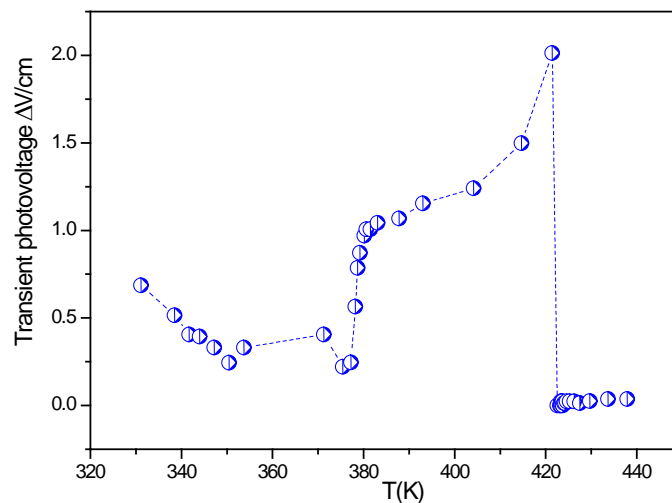


Figure 5 | Temperature dependence of the photovoltaic effect.

A clear non-monotonous dependence is observed near the each of the abovementioned transition temperatures. Notably a magnitude of the photovoltaic effect can be effectively tuned by temperature and reveals more than three times improvement before FE T_c and vanishes in the paraelectric temperature region. This behavior confirms the ferroelectric origin of the photovoltaicity that exists in

the electrically polar phase only. Moreover importantly, our results reveal photovoltaic effect tuning prospect connected to instabilities near the phase transitions where FE system can be governed by photostrictively correlated fluctuations of the polarization²².

In conclusion, we have discovered that a representative member of the piezoelectric family of PMN–32%PT complexes, the $\text{Pb}[(\text{Mg}_{1/3}\text{Nb}_{2/3})_{0.68}\text{Ti}_{0.32}]\text{O}_3$ crystal, exhibits photovoltaic properties in a wide temperature range. The electric field and temperature controllable photovoltages on the landmark archetype FE crystal should be regarded as key basic finding, clearly illustrating how charge separation relates to the FE properties and superposes to charge recombination. The patent separation between remnant and transient effects that have been shown here for the first time completes the profile of many recent photoelectric observations^{23,24,25,26,27} and is essential to realize and optimize FE based photovoltaic and optoelectronic devices. This study paves the way towards future investigations of bandgap tuning²⁸ in other compounds as well as composites of the same family to optimize composition-to-the-reported properties relationship. The photovoltaic properties and photopolarization effects that have been described herein can be generalized to many ferroelectric systems from the 21 piezoelectric crystal classes in which photovoltaic effects can occur²⁹. Especially, materials that can be used in tunnel junctions³⁰ and magnetic ferroelectric compounds with motivating optical functionalities^{31,32} becoming interesting candidates.

METHODS

The crystals were cut perpendicular to the [001] direction with the edges' orientations of [010] and [100]. The sample dimensions were $901.6\mu\text{m}\times 272\mu\text{m}\times 2160.6\mu\text{m}$ and the both electrodes were formed with the silver paste covering at the edges in the plane parallel to ZY (Fig. 1a). It has to be stressed that this geometry of the experiment was chosen to avoid light penetration through electrode to minimize light power loss and possible extrinsic contributions related to charge injection. The hysteresis loop of polarization versus electric field was taken at room temperature (RT) by using home-made quasi-static FE loop tracer previously employed to study ferroelectricity in multiferroics^{33,34,35}. The sample was irradiated with a 365 nm (3.4 eV) UV-LED with 30 nm spectral linewidth at 13.67mW of power in order to investigate the change in the FE polarization response. Measured by at room

temperature with thermal camera temperature has detected sample warming by 1.9K under illumination and such temperature change did not make any noticeable difference on FE loop. To measure polarization the sample was first warmed in darkness to 440K (above its Curie temperature of $T_c \sim 421\text{K}$) and then cooled at an applied electric field of 2.37kV/cm.

References

- ¹ Kreisel, J., Alexe, M. & Thomas, P. A. A photoferroelectric material is more than the sum of its parts. *Nat. Mater.* **11**, 260–260 (2012).
- ² Choi, T., Lee, S., Choi, Y. J., Kiryukhin, V. & Cheong, S.-W. Switchable Ferroelectric Diode and Photovoltaic Effect in BiFeO₃. *Science* **324**, 63–66 (2009).
- ³ Yi, H. T., Choi, T., Choi, S. G., Oh, Y. S. & Cheong, S.-W. Mechanism of the Switchable Photovoltaic Effect in Ferroelectric BiFeO₃. *Adv. Mater.* **23**, 3403–3407 (2011).
- ⁴ Butler, K. T., Frost, J. M. & Walsh, A. Ferroelectric materials for solar energy conversion: photoferroics revisited. *Energy Environ. Sci.* **8**, 838–848 (2015).
- ⁵ Paillard, C. *et al.* Photovoltaics with Ferroelectrics: Current Status and Beyond. *Adv. Mater.* **28**, 5153–5168 (2016).
- ⁶ Yang, S. Y. *et al.* Above-bandgap voltages from ferroelectric photovoltaic devices. *Nat. Nanotechnol.* **5**, 143–147 (2010).
- ⁷ Grinberg, I. *et al.* Perovskite oxides for visible-light-absorbing ferroelectric and photovoltaic materials. *Nature* **503**, 509–512 (2013).
- ⁸ Lopez-Varo, P. *et al.* Physical aspects of ferroelectric semiconductors for photovoltaic solar energy conversion. *Phys. Rep.* **653**, 1–40 (2016).
- ⁹ Nechache, R. *et al.* Bandgap tuning of multiferroic oxide solar cells. *Nat. Photonics* **9**, 61–67 (2015).
- ¹⁰ Takagi, K. *et al.* Ferroelectric and Photostrictive Properties of Fine-Grained PLZT Ceramics Derived from Mechanical Alloying. *J. Am. Ceram. Soc.* **87**, 1477–1482 (2004).
- ¹¹ Kundys, B. Photostrictive materials. *Appl. Phys. Rev.* **2**, 011301 (2015).
- ¹² Poosanaas, P., Dogan, A., Thakoor, S. & Uchino, K. Influence of sample thickness on the performance of photostrictive ceramics. *J. Appl. Phys.* **84**, 1508–1512 (1998).
- ¹³ Tu, C.-S. *et al.* Dielectric and photovoltaic phenomena in tungsten-doped Pb(Mg_{1/3}Nb_{2/3})_{1-x}Ti_xO₃ crystal. *Appl. Phys. Lett.* **88**, 032902 (2006).
- ¹⁴ PMN-PT compounds are commercially available from Crystal-gmbh (Germany).¹⁵ Park, J., Won, S. S., Ahn, C. W. & Kim, I. W. Ferroelectric Photocurrent Effect in Polycrystalline Lead-Free (K_{0.5}Na_{0.5})(Mn_{0.005}Nb_{0.995})O₃ Thin Film. *J. Am. Ceram. Soc.* **96**, 146–150 (2013).
- ¹⁶ Pintilie, L., Dragoi, C. & Pintilie, I. Interface controlled photovoltaic effect in epitaxial Pb(Zr,Ti)O₃ films with tetragonal structure. *J. Appl. Phys.* **110**, 044105 (2011).
- ¹⁷ Shrout, T. R., Chang, Z. P., Kim, N. & Markgraf, S. Dielectric behavior of single crystals near the (1-X) Pb(Mg_{1/3}Nb_{2/3})O₃-(x) PbTiO₃ morphotropic phase boundary. *Ferroelectr. Lett. Sect.* **12**, 63–69 (1990).
- ¹⁸ Guo, Y. *et al.* The phase transition sequence and the location of the morphotropic phase boundary region in (1-x)[Pb(Mg_{1/3}Nb_{2/3})O₃]-xPbTiO₃ single crystal. *J. Phys. Condens. Matter* **15**, L77 (2003).
- ¹⁹ Ueda, S., Tatsuzaki, I. & Shindo, Y. Change in the Dielectric Constant of SbSI Caused by Illumination. *Phys. Rev. Lett.* **18**, 453–454 (1967).
- ²⁰ Borkar, H. *et al.* Experimental evidence of electronic polarization in a family of photo-ferroelectrics. *RSC Adv.* **7**, 12842–12855 (2017).
- ²¹ Borkar, H. *et al.* Optically controlled polarization in highly oriented ferroelectric thin films. *Mater. Res. Express* **4**, 086402 (2017).
- ²² Wemple, S. H. & Di Domenico, M. Theory of the Elasto-Optic Effect in Nonmetallic Crystals. *Phys. Rev. B* **1**, 193–202 (1970).
- ²³ Moubah, R. *et al.* Photoelectric Effects in Single Domain BiFeO₃ Crystals. *Adv. Funct. Mater.* **22**, 4814–4818 (2012).
- ²⁴ Bhatnagar, A., Kim, Y. H., Hesse, D. & Alexe, M. Persistent Photoconductivity in Strained Epitaxial BiFeO₃ Thin Films. *Nano Lett.* **14**, 5224–5228 (2014).

-
- ²⁵ Bogle, K. *et al.* Optically modulated resistive switching in BiFeO₃ thin film. *Phys. Status Solidi A* **213**, 2183–2188 (2016).
- ²⁶ Bai, Z. *et al.* The abnormal photovoltaic effect in BiFeO₃ thin films modulated by bipolar domain orientations and oxygen-vacancy migration. *Appl. Phys. A* **123**, 561 (2017).
- ²⁷ Fan, H. *et al.* Large electroresistance and tunable photovoltaic properties of ferroelectric nanoscale capacitors based on ultrathin super-tetragonal BiFeO₃ films. *J. Mater. Chem. C* **5**, 3323–3329 (2017).
- ²⁸ Matsuo, H., Noguchi, Y. & Miyayama, M. Gap-state engineering of visible-light-active ferroelectrics for photovoltaic applications. *Nat. Commun.* **8**, 207 (2017).
- ²⁹ von Baltz, R. & Kraut, W. Theory of the bulk photovoltaic effect in pure crystals. *Phys. Rev. B* **23**, 5590–5596 (1981).
- ³⁰ Hu, W. J., Wang, Z., Yu, W. & Wu, T. Optically controlled electroresistance and electrically controlled photovoltage in ferroelectric tunnel junctions. *Nat. Commun.* **7**, 10808 (2016).
- ³¹ Manz, S. *et al.* Reversible optical switching of antiferromagnetism in TbMnO₃. *Nat. Photonics* **10**, 653–656 (2016).
- ³² Mettout, B. & Gisse, P. Theory of the photovoltaic and photo-magneto-electric effects in multiferroic materials. *Ferroelectrics* **506**, 93–110 (2017).
- ³³ Kundys, B., Simon, C. & Martin, C. Effect of magnetic field and temperature on the ferroelectric loop in MnWO₄. *Phys. Rev. B* **77**, 172402 (2008).
- Martin, N. Nguyen, and Ch. Simon, *Appl. Phys. Lett.* **92**, 112905 (2008)
- ³⁴ Kundys, B., Maignan, A., Martin, C., Nguyen, N. & Simon, C. Magnetic field induced ferroelectric loop in Bi_{0.75}Sr_{0.25}FeO_{3-δ}. *Appl. Phys. Lett.* **92**, 112905 (2008).
- ³⁵ Kundys, B. *et al.* Multiferroicity and hydrogen-bond ordering in (C₂H₅NH₃)₂CuCl₄ featuring dominant ferromagnetic interactions. *Phys. Rev. B* **81**, 224434 (2010).